Effect of Mg²⁺ ions co-doping on luminescence and defects formation processes in Gd₃(Ga,Al)₅O₁₂:Ce single crystals

V. Babin [a], P. Bohacek [a], L. Grigorjeva [b], M. Kučera [c], M. Nikl [a], S. Zazubovich [d, *], A. Zolotarjovs [b]

[a] Institute of Physics AS CR, Cukrovarnicka 10, 16200, Prague, Czechia
[b] Institute of Solid State Physics, University of Latvia, Kengaraga 8, Riga, LV-1063, Latvia
[c] Charles University, Faculty of Mathematics and Physics, Ke Karlovu 5, 12116, Prague, Czechia
[d] Institute of Physics, University of Tartu, W. Oswaldi 1, 50411, Tartu, Estonia

A B S T R A C T

Photo- and radioluminescence and thermally stimulated luminescence characteristics of Ce³⁺ - doped and Ce³⁺, Mg²⁺ co-doped Gd₃(Ga,Al)₅O₁₂ (GAGG) single crystals of similar composition are investigated in the 9–500 K temperature range. The Ce³⁺ - related luminescence spectra and the photoluminescence decay kinetics in these crystals are found to be similar. Under photoexcitation in the Ce³⁺ - and Gd³⁺ - related absorption bands, no prominent rise of the photoluminescence intensity in time is observed neither in GAGG:Ce,Mg nor in GAGG:Ce crystals. The afterglow is strongly reduced in GAGG:Ce,Mg as compared to GAGG:Ce, and the afterglow decay kinetics is much faster. Co-doping with Mg²⁺ results in a drastic decrease of the thermally stimulated luminescence (TSL) intensity in the whole investigated temperature range and in the appearance of a new complex Mg²⁺ - related TSL glow curve peak around 285 K. After irradiation in the Ce³⁺ - related 3.6 eV absorption band, the TSL intensity in GAGG:Ce,Mg is found to be comparable with that in the GAGG:Ce epitaxial film of similar composition. The Mg²⁺ - induced changes in the concentration, origin and structure of the crystal lattice defects and their influence on the scintillation characteristics of GAGG:Ce,Mg are discussed.

© 2017 Elsevier B.V. All rights reserved.

1. Introduction

In recent years, the Ce - doped Gd₃Ga$_x$Al$_{5-x}$O₁₂ (GAGG:Ce) single crystals, ceramics and epitaxial films with different Ga contents were intensively studied as promising scintillator materials for their application in medical imaging because of their extremely high light yield, good energy resolution, relatively high density (6.63 g/cm³), fast scintillation response, and high radiation stability and hardness [1–24]. Single crystals of Gd₃Ga$_x$Al$_{5-x}$O₁₂:Ce prepared by the micro-pulling down method were first reported in Ref. [1]. Their scintillation characteristics were found to be dependent on the Ga concentration. For the crystal with x = 3, the light yield of ≈ 42 000 photons/MeV, the dominating decay time of ≈ 53 ns, and the energy resolution of 8.3%@662 keV were obtained. With the decreasing Ga content, the light yield and energy resolution were found to improve, but the decay time increases. The

first Gd₃Ga₃Al₂O₁₂:Ce single crystal grown by the Czochralski method with the light yield of 46 000 photons/MeV and energy resolution of 4.9%@662 keV was reported in Ref. [2]. Recently, an extremely high light yield of 58 000 photon/MeV and the best energy resolution of 4.2%@662 keV were obtained for the single crystals of Gd₃Ga$_x$Al$_{5-x}$O₁₂:Ce with x = 2.7 and x = 2.4, respectively, also grown by the Czochralski method [11]. Due to these characteristics, GAGG:Ce was considered as a promising scintillator for the PET application [2].

However, single crystals of GAGG:Ce showed relatively intense afterglow and thermally stimulated luminescence (TSL) due to the presence of antisite- and vacancy-related defects which act as effective traps for electrons. The preparation of Ce - doped garnets at much lower temperatures by the liquid phase epitaxy (LPE) method allowed to noticeably decrease the concentration of these defects (see, e.g., [25–27]). Scintillation characteristics of the LPE films of GAGG:Ce prepared with the use of a BaO-B₂O₃-BaF₂ flux were studied in Ref. [18], and their photo- and thermally stimulated luminescence were recently reported in Refs. [23,24].

* Corresponding author.
E-mail address: svea@ut.ee (S. Zazubovich).

The studies of $Gd_3Ga_xAl_{5-x}O_{12}$:Ce showed that the increasing Ga content results in the high-energy shift of the Ce^{3+} - related $5d_1 - 4f$ emission band and the lowest-energy $4f - 5d_1$ absorption (excitation) band as well as in the low-energy shift of the $4f - 5d_2$ excitation band [6,24]. The Stokes shift slightly increases as well. The decrease of both the crystal field strength and the band gap of the host material was observed (see, e.g. [4,6], and references therein). According to [6], the activation energy of thermal quenching of the $5d_1 - 4f$ emission determined from the temperature dependence of the luminescence decay time decreases from $E_q \approx 0.6$ eV for x = 0, to $E_q \approx 0.5$ eV for x = 1, to $E_q \approx 0.25$ eV for x = 3 and to $E_q \approx 0.1$ eV for x = 4. In Ref. [23], the energy distance between the excited $5d_1$ level of Ce^{3+} and the bottom of the conduction band was directly determined by the TSL method and found to decrease with the increasing Ga content.

Recently it was found that a considerable improvement of scintillation characteristics can be also achieved by the co-doping of GAGG:Ce crystals with divalent alkali-earth ions, e.g., with Mg^{2+} or Ca^{2+} [5,14,15,19]. Indeed, the studies [5,14] showed that the Ca^{2+} co-doping of Czochralski grown GAGG:Ce results in a strong reduction of the afterglow and TSL at T < 300 K. It also results in a noticeable improvement of timing characteristics of the material which is very important for PET applications. However the light yield of GAGG:Ce,Ca was found to be considerably lower as compared to GAGG:Ce. Besides, a new intense TSL peak at 390 K appears at the TSL glow curve of GAGG:Ce,Ca indicating the formation of deep electron traps. The Mg^{2+} co-doping was found to have much better influence on the scintillation characteristics of GAGG:Ce as compared with the Ca^{2+} co-doping [15,19]. Indeed, the GAGG:Ce,Mg crystals showed considerable improvement of the timing performance (much faster decay and rise times of the scintillation pulse with consequent improvement of the coincidence time resolution) and comparatively smaller light output decrease with the increasing Mg concentration.

It was also found that co-doping of various Ce - doped materials with divalent ions (M^{2+}) results in the change of cerium valence state from Ce^{3+} to Ce^{4+} (see, e.g. [28—30], and references therein). Both the Ca^{2+} and Mg^{2+} co-doping was found to stimulate the appearance of Ce^{4+} centers also in GAGG:Ce crystals [5,14,15,19]. The presence of Ce^{4+} is manifested by appearance of a broad absorption band in the 4—6 eV energy range caused by an electon transfer from the valence band to the ground 4f state of the Ce^{4+} ion. In the crystal where the Ca content is two times larger as compared with the Ce content, the Ce^{4+} centers considerably outweigh the Ce^{3+} centers [14]. Only the presence of such excellent electron traps as the Ce^{4+} ions in the M^{2+} co-doped GAGG:Ce crystals can explain a strong suppression of slow components in the scintillation decay, since it prevents electron capture at various intrinsic defects and provides an alternative channel for fast radiative recombinations (for more details, see, e.g. [14,15,19], and references therein).

However, the mechanism of processes resulting in the light yield reduction in the co-doped crystals as well as the reasons of different influence of the Ca^{2+} and Mg^{2+} co-doping on the light yield reduction were not understood. The TSL characteristics as well as the origin and parameters of the traps in GAGG:Ce,Mg were not studied. Therefore, it was of great interest to understand the influence of Mg^{2+} ions on the defect structure, characteristics of the electrons and hole traps, energy levels of Ce^{3+} and Ce^{4+} ions, and recombination processes in GAGG:Ce. In the present work, the characteristics of the photo- and X-ray excited luminescence and thermally stimulated luminescence of GAGG:Ce and GAGG:Ce,Mg single crystals of approximately the same composition prepared by the Czochralski method are investigated in a wide temperature range (9—500 K) and compared. The characteristics of the single crystals are compared with the corresponding characteristics of the GAGG:Ce epitaxial films studied in Refs. [18,23,24]. Absorption and radioluminescence spectra of the investigated single crystals, as well as their scintillation characteristics measured at room temperature have been reported in Ref. [19].

2. Experimental procedure

Single crystals of GAGG:Ce and GAGG:Ce,Mg were grown using the Czochralski technique (for more details, see Ref. [19]). The composition of the samples was analyzed using an electron probe microanalysis and was found to be $Gd_{3.027}Ga_{2.831}Al_{2.135}O_{12}$:$Ce_{0.0071}$ in GAGG:Ce and $Gd_{3.046}Ga_{2.694}Al_{2.253}O_{12}$:$Ce_{0.005}Mg_{0.0022}$ in GAGG:Ce,Mg. Thus, with respect to Gd, the Ce concentration was 0.237 at.% in GAGG:Ce and 0.167 at.% in GAGG:Ce,Mg. The Mg concentration in the GAGG:Ce,Mg crystal was 0.073 at.%. The $Gd_{3.02}Ga_{2.7}Al_{2.26}O_{12}$:$Ce_{0.02}$ (5LGB5) epitaxial film was grown in Ref. [18] by isothermal dipping liquid phase epitaxy from BaO-B_2O_3-BaF_2 flux onto Czochralski grown $Gd_3Ga_5O_{12}$ substrate. The concentration of Ce in the film was about 0.7 at.% and the film thickness, of 25.5 μm. The above-mentioned samples were used for the photoluminescence, X-ray-excited luminescence and thermaly stimulated luminescence studies. For the investigations of the photoluminescence decay kinetics, the GAGG:Ce ($Gd_{3.047}Ce_{0.0041}$-$Ga_{2.695}Al_{2.254}O_{12}$) and GAGG:Ce,Mg ($Gd_{3.011}Ce_{0.0044}Mg_{0.0021}$-$Ga_{2.644}Al_{2.339}O_{12}$) single crystals [19] and the GAGG:Ce epitaxial film ($Gd_{3.04}Ga_{2.98}Al_{1.96}O_{12}$:$Ce_{0.02}$ - 5LGB7) grown onto $Y_3Ga_5O_{12}$ substrate [18] were used.

The steady-state emission and excitation spectra in the 90—500 K temperature range were measured using a setup, consisting of the LOT - ORIEL xenon lamp (150 W) and two monochromators (SF - 4 and SPM - 1). The luminescence was detected by a photomultiplier (FEU - 39 or FEU - 79) connected with an amplifier and recorder.

Luminescence decay curves I(t) were measured with a custom made 5000 M model of Horiba Jobin Yvon spectrofluorometer under excitation with a nanosecond coaxial hydrogen-filled flashlamp ($E_{exc} = 4.59$ eV) or nanoLED sources ($E_{exc} = 3.66$ eV and 2.74 eV) (both IBH Scotland) with pulse durations around 1 ns. The shortest available time range was used (212.78 ns), and the corresponding time-per-channel was 0.208 ns. The detection was performed with a photon counting TBX-04 photomultiplier module (IBH Scotland). The I(t) curves were measured for the Ce^{3+} - related 2.38 eV emission. A convolution procedure (SpectraSolve software package, Ames photonics) was applied to extract true decay times using the multiexponential approximation.

The photoluminescence characteristics were measured with the use of nitrogen cryostats.

The X-ray excited luminescence and afterglow spectra were measured at 9 K after a crystal was irradiated with the X-ray tube (40 kV, 15 mA) for 10 min to achieve the intensity saturation. The luminescence was detected using Andor Shamrock B-303i spectrograph coupled with Andor DU-401A-BV CCD camera. In addition, HAMAMATSU H2859 photomultiplier tube was used to gain extra sensitivity.

Thermally stimulated luminescence glow curves $I_{TSL}(T)$ were measured with a heating rate of 0.2 K/s at two different setups. At the first setup, the TSL glow curves were measured in the 90—500 K temperature range after selective UV irradiation of the crystals at different temperatures T_{irr} with different irradiation photon energies E_{irr}. A crystal located in a nitrogen cryostat was irradiated with the LOT - ORIEL xenon lamp (150 W) through a monochromator SF-4. The spectral width of the monochromator slit did not exceed 5 nm. The TSL glow curves were measured with the monochromator SPM-1 and detected with the photomultiplier
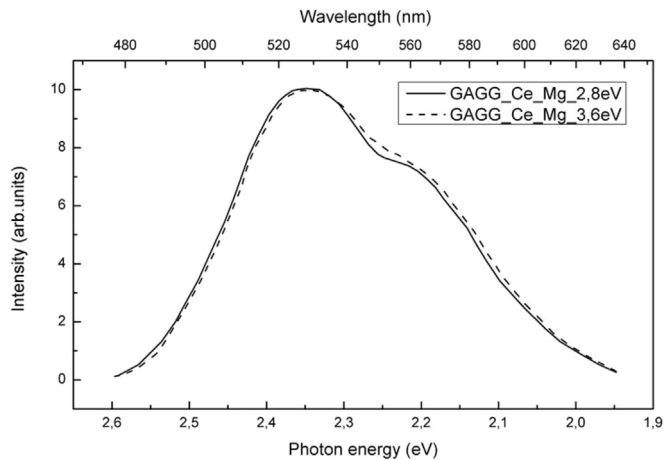
Fig. 1. Uncorrected emission spectra of GAGG:Ce,Mg measured at 85 K under excitation in the Ce^{3+} - related $4f-5d_1$ (2.8 eV; solid line) and $4f-5d_2$ (3.6 eV; dashed line) absorption bands. The spectral width of the monochromator slits was 3.5 nm.

FEU-39 and recorder. For each TSL glow curve peak, the TSL peak creation spectrum, i.e., the dependence of the maximum TSL intensity (I_{TSL}^{max}) on the irradiation photon energy E_{irr}, was measured. From the dependence of the maximum TSL intensity (I_{TSL}^{max}) on the irradiation temperature T_{irr}, the activation energy E_a for the TSL peak creation was determined. To determine the trap depth E_t corresponding to each TSL peak, the partial cleaning method was used (for more details, see, e.g. [31], and references therein). The crystal, irradiated at the temperature T_{irr}, was cooled down to 90 K, heated up to a temperature T_{stop}, then quickly cooled down to 90 K and the TSL glow curve was recorded. In the next cycle, the same procedure was repeated for the different temperature T_{stop}, etc. From the slope of the $ln(I_{TSL})$ as a function of the reverse temperature (1/T), the E_t value was calculated.

At the second setup, the TSL glow curves were measured in the 9–300 K temperature range after X-ray irradiation of the crystals with the X-ray tube (40 kV, 15 mA) for 15 min. The luminescence was detected using Andor Shamrock B-303i spectrograph coupled to Andor DU-401A-BV CCD camera. In addition, HAMAMATSU H2859 photomultiplier tube was used to gain extra sensitivity. Trap depths were determined using fractional glow technique [32].

3. Experimental results and discussion

As mentioned above, co-doping of various Ce - doped materials with divalent ions (M^{2+}) results in the change of cerium valence state from Ce^{3+} to Ce^{4+}. For the local excess charge and volume compensation, the formation of Ce^{4+} and M^{2+} pairs can be possible in some materials. For example, the presence of the $\{Ce^{4+} - Pb^{2+}\}$ centers in the lead-containing Y_2SiO_5:Ce and Lu_2SiO_5:Ce epitaxial films was found in Ref. [28]. The formation of such centers could influence the luminescence characteristics of the material, in particular, the characteristics of the electron recombination luminescence (ERL) which could arise from the recombination of electrons with single Ce^{4+} ions and with the $\{Ce^{4+} - M^{2+}\}$ centers. This effect could appear in the shift of the luminescence spectrum and in the change of the decay kinetics and temperature dependence of the luminescence intensity in the M^{2+} co-doped materials as compared to the M^{2+} free ones. We have also suggested that the difference in the activation energies of the luminescence thermal quenching reported in Ref. [14] can be explained by the fact that the X-ray excited ERL arises in these crystals from the recombination of electrons with different Ce^{4+} - type centers: with single Ce^{4+}

centers in GAGG:Ce but with both the Ce^{4+} and the $\{Ce^{4+} - Ca^{2+}\}$ centers, in GAGG:Ce,Ca. Indeed, in the GAGG:Ce, Ca crystal with the largest (0.4 at. %) Ca concentration, practically all Ce ions are in a tetravalent form [14] and, owing to a large Ca^{2+} content, the number of the $\{Ce^{4+} - Ca^{2+}\}$ pairs could be noticeable. In this case, the difference in the activation energies reported in Ref. [14] could be caused by different energy distances between the conduction band and the relaxed $5d_1$ state of Ce^{3+} and $\{Ce^{3+} - Ca^{2+}\}$ centers, indicating a noticeable influence of Ca^{2+} on the energy levels of Ce^{3+}.

According to [30], the co-doping of $Lu_3Al_5O_{12}$:Ce with Mg^{2+} stimulates the formation of paramagnetic O^- - type hole centers. We have suggested that the same effect could take place also in GAGG:Ce,Mg. In principle, the recombination of electrons with the Mg^{2+} - stabilized O^- hole centers could result in the appearance of the localized exciton luminescence (similar to that observed, e.g., in Y_2SiO_5:Ce and Lu_2SiO_5:Ce crystals [37]).

Taking into account the above-mentioned data, we tried to detect the above-mentioned exciton luminescence as well as the presence of Ce^{3+} or Ce^{4+} ions perturbed by Mg^{2+} ions in the GAGG:Ce,Mg crystal. For that, we carefully compared the low-temperature emission and excitation spectra, the luminescence decay kinetics, as well as the temperature dependences of the luminescence intensity and decay times measured for the GAGG:Ce and GAGG:Ce,Mg single crystals under photoexcitation in the Ce^{3+} - related absorption bands. We also compared the photoluminescence characteristics of GAGG:Ce,Mg measured at 90 K under excitation in the $4f - 5d_1$ band of Ce^{3+}, where only the intra-centre Ce^{3+} emission can be excited, and under excitation in the $4f - 5d_2$ band, where the ERL could also appear due to the recombination of electrons, optically released to the conduction band, with the Ce^{4+}, $\{Ce^{4+} - Mg^{2+}\}$, and $\{O^- - Mg^{2+}\}$ - type hole centers. Besides, the characteristics of the ERL of GAGG:Ce and GAGG:Ce,Mg have been compared also under X-ray excitation of the investigated crystals at 9 K.

3.1. Photoluminescence of GAGG:Ce and GAGG:Ce,Mg

No noticeable difference was found in the photoluminescence spectra of the GAGG:Ce and GAGG:Ce,Mg crystals measured with very narrow slits. A small (≈ 0.01 eV) lower-energy shift of the GAGG:Ce,Mg spectrum with respect to the GAGG:Ce spectrum can
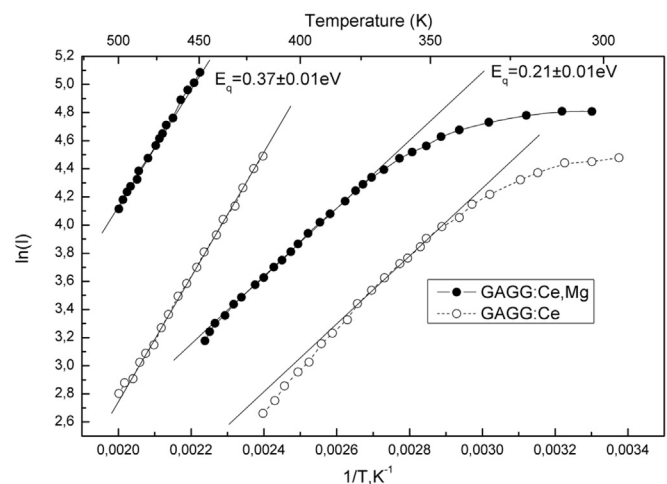

Fig. 2. The $lnI - 1/T$ dependences presented for the GAGG:Ce (open circles) and GAGG:Ce,Mg (filled circles) single crystals under excitation in the Ce^{3+} - related $4f-5d_1$ absorption band.
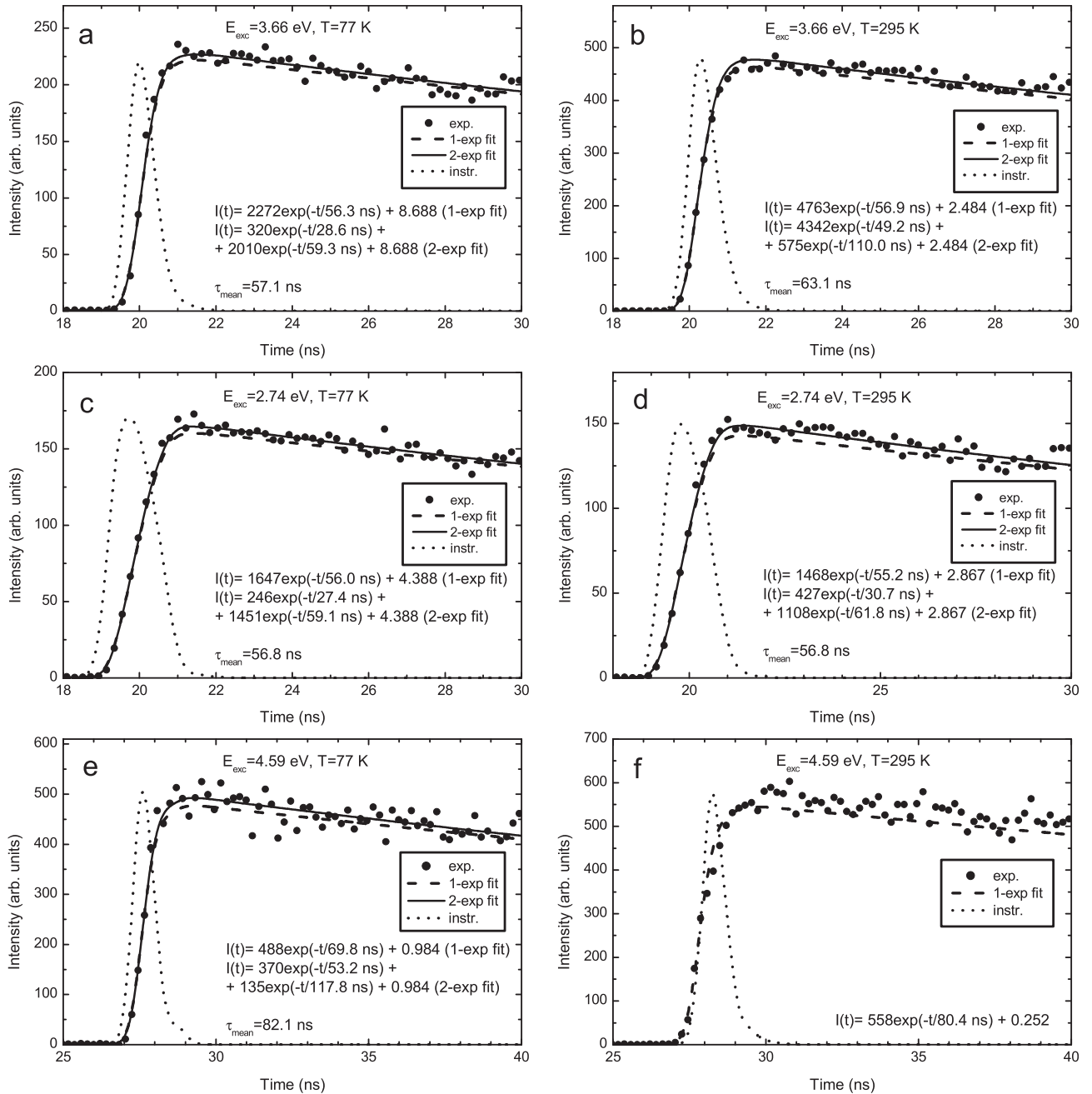
Fig. 3. Decay kinetics of the Ce^{3+}-related emission of the single crystal of GAGG:Ce ($Gd_{3.047}Ce_{0.0041}Ga_{2.695}Al_{2.254}O_{12}$) measured at 77 K and 295 K under excitation in the (a, b) Ce^{3+}-related $4f - 5d_2$ ($E_{exc} = 3.66$ eV) and (c, d) $4f - 5d_1$ ($E_{exc} = 2.74$ eV) absorption bands and (e, f) in the Gd^{3+}-related absorption band ($E_{exc} = 4.59$ eV).

be caused by a smaller Ga content in this crystal, see Refs. [6,24]. No noticeable difference was found in the photoluminescence spectra of GAGG:Ce,Mg measured under the $4f - 5d_1$ and $4f - 5d_2$ excitations (Fig. 1).

No noticeable difference was also observed in the temperature dependences of the $5d_1 - 4f$ luminescence intensity measured for GAGG:Ce and GAGG:Ce,Mg (Fig. 2). At the temperatures T < 280 K, the emission intensity is slightly decreasing due to the decreasing probability of the $4f - 5d_1$ absorption transitions. At higher temperatures, the intensity decrease with the activation energies $E_q = 0.20-0.22$ eV and $E_q \approx 0.37 \pm 0.02$ eV is observed in the 350−400 K and 400−500 K temperature ranges, respectively. As it will be shown in Section 3.3, the former decrease is caused by the

thermally stimulated release of electrons from the $5d_1$ level of Ce^{3+} into the conduction band (the Ce^{3+} ionization). The latter decrease should be caused by some other process. In the GAGG:Ce epitaxial film of approximately the same composition (5LGB5), the activation energy of the luminescence thermal quenching in the 400−500 K temperature range has been found to be $E_q = 0.56$ eV [23]. Therefore, much smaller activation energy $E_q \approx 0.37 \pm 0.02$ eV obtained for the same temperature range in the GAGG:Ce and GAGG:Ce,Mg single crystals cannot arise from the nonradiative $5d_1 - 4f$ transitions of Ce^{3+} ions but should be caused by some other, defect-related, process which is strongly suppressed in the epitaxial film. The activation energy values of 0.36 eV and 0.42 eV reported for GAGG:Ce in Refs. [33] and [5], respectively, and obtained from the
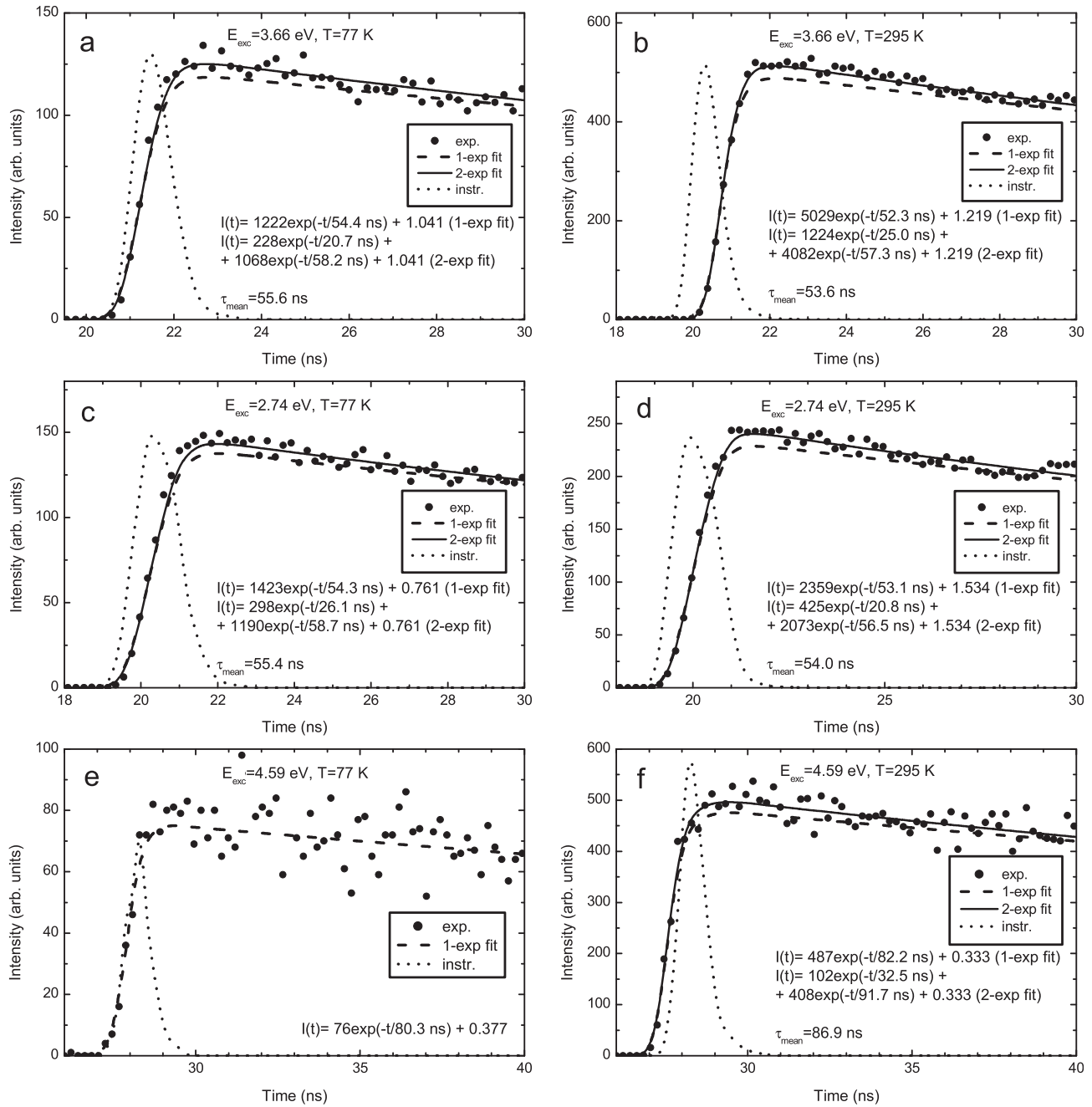
Fig. 4. Decay kinetics of the Ce^{3+}-related emission of the single crystal of GAGG:Ce,Mg ($Gd_{3.011}Ce_{0.0044}Mg_{0.0021}Ga_{2.644}Al_{2.339}O_{12}$) obtained at 77 K and 295 K under excitation in the (a, b) Ce^{3+}-related $4f - 5d_2$ ($E_{exc} = 3.66$ eV) and (c, d) $4f - 5d_1$ ($E_{exc} = 2.74$ eV) absorption bands and (e, f) in the Gd^{3+}-related absorption band ($E_{exc} = 4.59$ eV).

temperature dependences of the emission intensity and decay time, might be characteristic just for the latter process but not for the Ce^{3+} ionization. These data confirm the conclusion made in Ref. [23]: the true activation energy (E_a) value for the thermally stimulated $5d_1 - CB$ transitions can be obtained only from the studies of the defects creation processes under irradiation of the crystal in the Ce^{3+} - related $4f - 5d_1$ or $4f - 5d_2$ absorption bands. Besides, since the E_a value strongly depends on the Ga content in the multicomponent garnets [23], another reason of large E_q values obtained in Refs. [5,33] can be caused by smaller true Ga concentration in the investigated crystals (compared to the value known in the melt).

As mentioned above, the GAGG:Ce co-doping with Mg^{2+} results

in a noticeable shortening of the scintillation decay and rise times (for more details, see Ref. [19]). Therefore, it was of interest to investigate the influence of Mg^{2+} on the photoluminescence decay kinetics of GAGG:Ce. In Figs. 3 and 4, the initial parts of the decay curves I(t) of the Ce^{3+} - related emission of GAGG:Ce and GAGG:-Ce,Mg single crystals measured at different experimental conditions (shown in the legends) are presented. For comparison, the initial parts of the decay curves obtained for the GAGG:Ce epitaxial film are also shown in Fig. 5. The fits of an experimental decay curve with one or two exponential components are shown by lines. In case of the two-exponential approximation, instead of the decay time τ, the mean time τ_{mean} is used defined by the equation [34]:
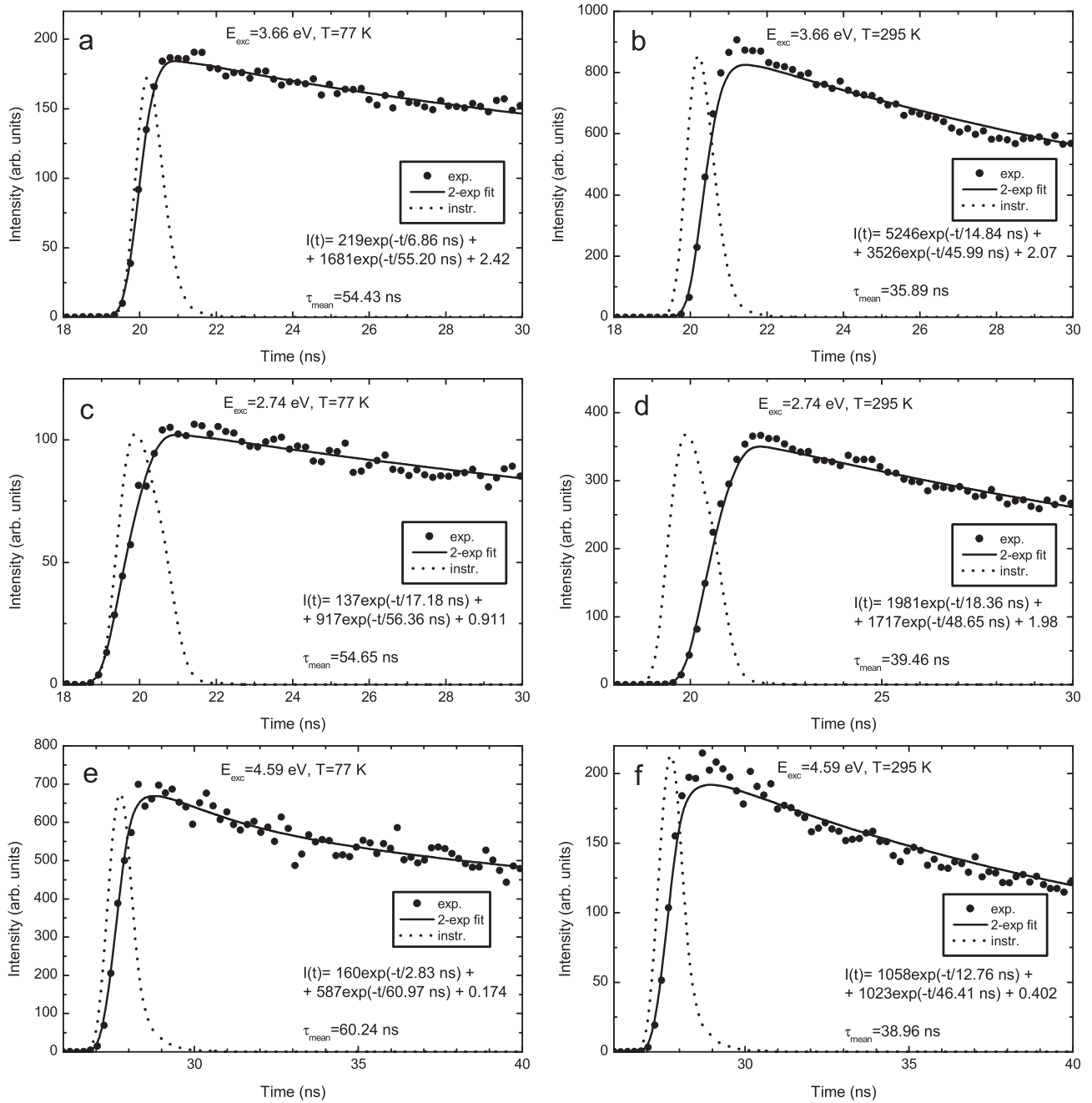
Fig. 5. Decay kinetics of the Ce^{3+}-related emission of the GAGG:Ce epitaxial film ($Gd_{3.04}Ga_{2.98}Al_{1.96}O_{12}$:$Ce_{0.02}$ - 5LGB7) obtained at 77 K and 295 K under excitation in the (a, b) Ce^{3+}-related $4f - 5d_2$ ($E_{exc} = 3.66$ eV) and (c, d) $4f - 5d_1$ ($E_{exc} = 2.74$ eV) absorption bands and (e, f) in the Gd^{3+}-related absorption band ($E_{exc} = 4.59$ eV).

Table 1

Decay times (ns) of the Ce^{3+}-related emission obtained for the GAGG:Ce ($Gd_{3.047}Ce_{0.0041}Ga_{2.695}Al_{2.254}O_{12}$) and GAGG:Ce,Mg ($Gd_{3.011}Ce_{0.0044}Mg_{0.0021}Ga_{2.644}Al_{2.339}O_{12}$) single crystals and the GAGG:Ce epitaxial films of different compositions ($Gd_{3.04}Ga_{2.98}Al_{1.96}O_{12}$:$Ce_{0.02}$ - 5LGB7 and $Gd_{3.02}Ga_{2.24}Al_{2.72}O_{12}$:$Ce_{0.02}$ - 5LGB2) under excitation in the Ce^{3+}-related $4f - 5d_2$ ($E_{exc} = 3.66$ eV) and $4f - 5d_1$ ($E_{exc} = 2.74$ eV) absorption bands and in the Gd^{3+}-related absorption band ($E_{exc} = 4.59$ eV). The data for the 5LGB2 film are taken from Ref. [23] for comparison. The first number is the decay time obtained in the 1-exponential approximation and the second number is the mean time (τ_{mean}) obtained in the 2-exponential approximation, see Figs. 3–5.

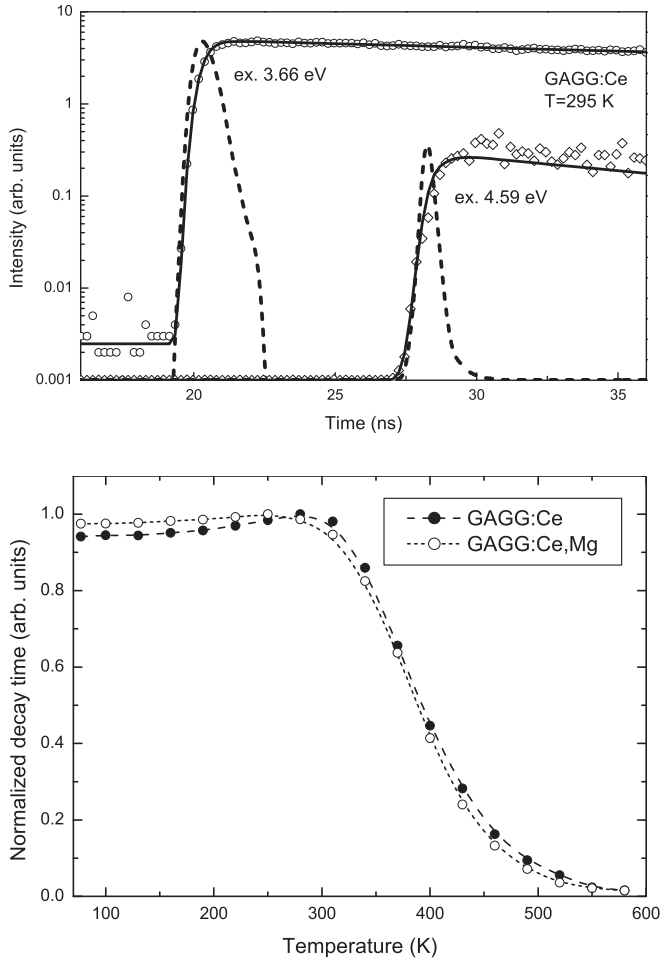| Sample/E_{exc}	T = 77 K			T = 295 K		
	3.66 eV	2.74 eV	4.59 eV	3.66 eV	2.74 eV	4.59 eV
GAGG:Ce	56.3; 57.1	56.0; 56.8	69.8; 82.1	56.9; 63.1	55.2; 56.8	80.4
GAGG:Ce,Mg	54.4; 55.6	54.3; 55.4	80.3	52.3; 53.6	53.1; 54.0	82.2; 86.9
5LGB7 film	54.4	54.7	60.2	35.9	39.5	39.0
5LGB2 flm	55.8	56.0	64.4	44.6	48.0	51.7

Fig. 6. (a) Initial part of the photoluminescence decay curves measured at 295 K for the visible Ce^{3+} emission of the GAGG:Ce single crystal under excitation in the $4f - 5d_2$ (E_{exc} = 3.66 eV) absorption band of Ce^{3+} and in the Gd^{3+} - related absorption band; E_{exc} = 4.59 eV. (b) Normalized temperature dependences of the luminescence decay times measured under excitation in the Ce^{3+} - related $4f - 5d_1$ absorption band of GAGG:Ce (filled circles) and GAGG:Ce,Mg (empty circles); E_{exc} = 2.72 eV.
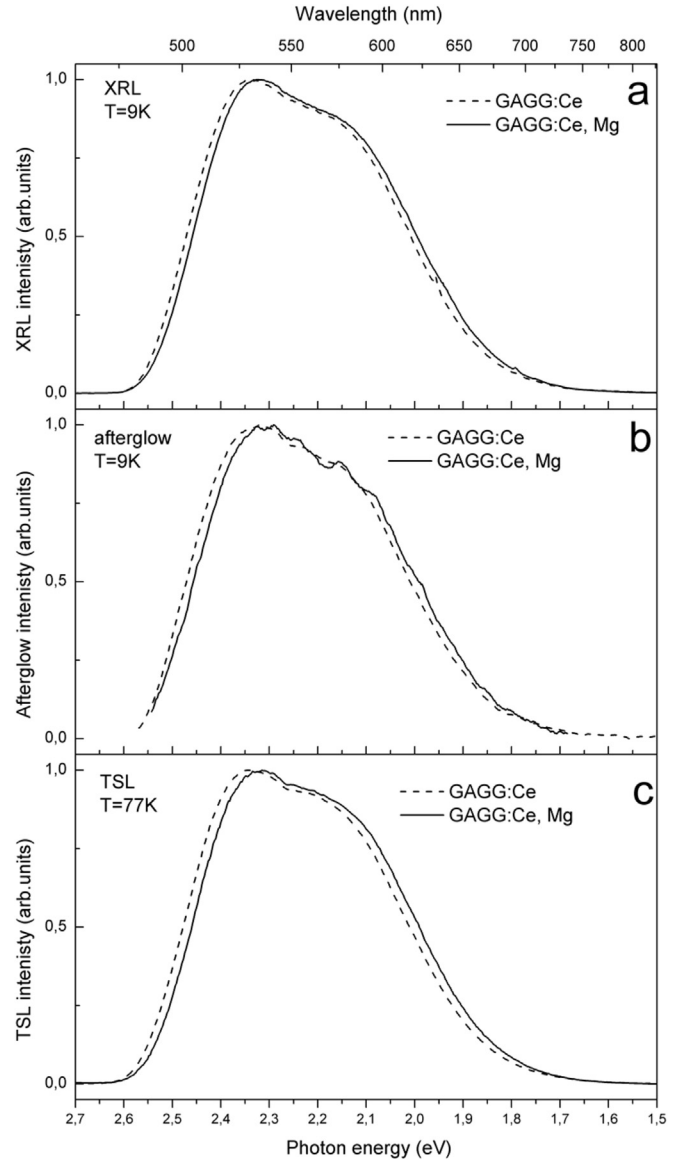

Fig. 7. Corrected spectra of the (a) X-ray excited luminescence, (b) afterglow, and (c) thermally stimulated luminescence measured at the same conditions for the GAGG:-Ce,Mg (solid line) and GAGG:Ce (dashed line) crystals. The spectral width of the monochromator slits was 1.1 nm.

$$\tau_{mean} = \sum A_i \tau_i^2 \Big/ \sum A_i \tau_i, \qquad (1)$$

where τ_i are the decay times of the single-exponential components and A_i are the corresponding initial intensities. The τ and τ_{mean} values are presented in Table 1.

The analysis of the obtained data has shown that all the I(t) curves presented in Figs. 3–5 are similar. The coinciding decay curves are observed even under excitation in the 4f - 5d$_2$ absorption band, where the ionization of Ce^{3+} takes place and electron and hole centers are created, and under excitation at 77 K in the 4f - 5d$_1$ absorption band (Fig. 3c and Fig. 5c), where no ionization is possible. In the latter case, only the intra-centre luminescence of Ce^{3+} is excited. In all the samples studied, no prominent photoluminescence intensity rise is observed under all considered excitation conditions. It should be especially noted that, unlike in the scintillation decay [19], no noticeable intensity rise is observed even for the single crystal of GAGG:Ce. As an example, the initial parts of the I(t) curves, measured for this crystal at 295 K under excitation in the 4f-5d$_2$ absorption band of Ce^{3+} and in the Gd^{3+} - related band, are demonstrated in more detail in Fig. 6a. However, in case the rise time value is below 1 nanosecond, its observation

could be hampered by the time resolution limits of our experiment.

Temperature dependences of the luminescence decay times in the GAGG:Ce and GAGG:Ce,Mg crystals are also practically coinciding (Fig. 6b). Similarly to the temperature dependences of the emission intensity (Fig. 2), two exponential stages with the activation energies around 0.21 eV and 0.37 eV can be separated in the 360–410 K and 450–520 K temperature ranges.

The comparison of the data obtained for the single crystals of GAGG:Ce and GAGG:Ce,Mg under excitation in the 4f - 5d absorption bands of Ce^{3+} allows us to conclude that, unlike in the scintillation decay [19], the influence of Mg co-doping on the decay kinetics of the Ce^{3+} - related photoluminescence is negligible (see Figs. 3 and 4 and Table 1).

Relatively short decay times observed at 295 K for the 5LGB7 film (Fig. 5) are caused by relatively large Ga content in this film. Due to that, the thermal quenching of the Ce^{3+} - related emission caused by the Ce^{3+} ionization takes place at lower temperatures
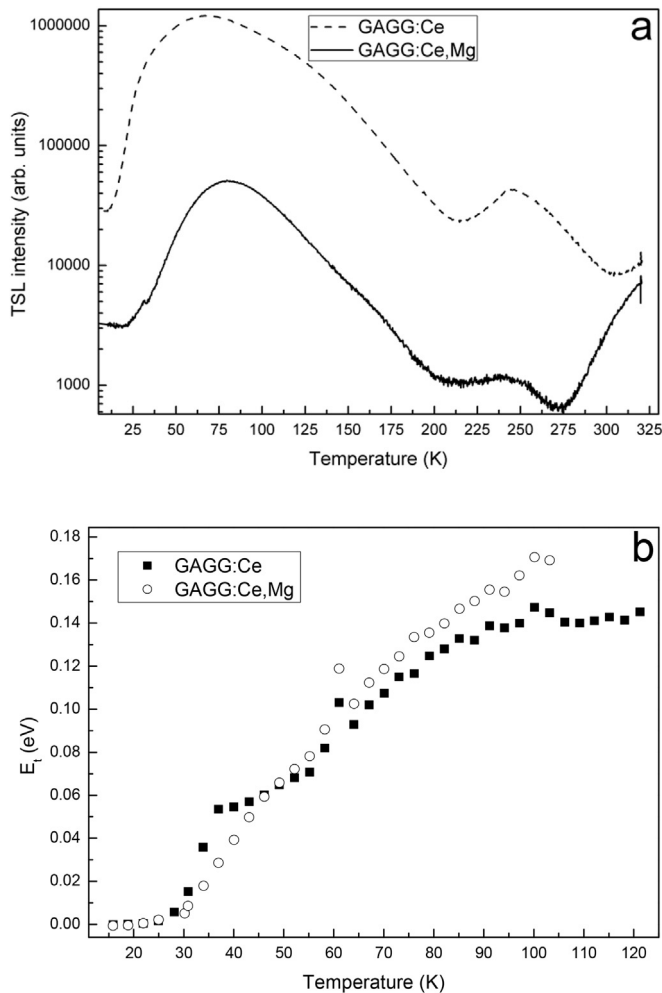
Fig. 8. (a) TSL glow curves of the X-ray irradiated at 9 K GAGG:Ce, Mg (solid line) and GAGG:Ce (dashed line) single crystals measured at the same conditions in the 9—300 K temperature range. (b) Trap depths for the 9—125 K temperature range acquired using fractional glow technique.
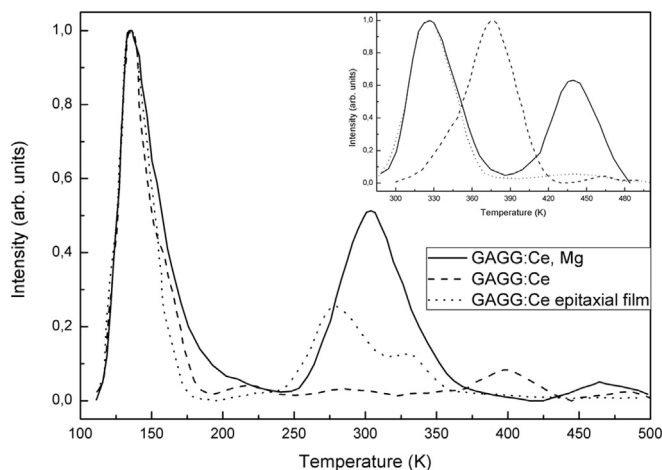

Fig. 9. TSL glow curves (normalized at 114 K) measured in the 90—500 K temperature range for the GAGG:Ce,Mg (solid line) and GAGG:Ce (dashed line) single crystals and the GAGG:Ce epitaxial film (dotted line) irradiated at 85 K in the Ce^{3+} - related 4f − 5d$_2$ absorption band (3.6 eV). In the inset, the TSL glow curves (normalized at maximum intensity) measured after irradiation of the same samples at 295 K in the Ce^{3+} - related 4f − 5d$_1$ absorption band (2.75 eV).

[24].

Under excitation in the Gd^{3+} - related absorption band ($E_{exc} = 4.59$ eV), the expected slower decay kinetics of the Ce^{3+} emission is observed, which is caused by the effective Gd^{3+} - Ce^{3+} energy transfer processes (for more details, see Ref. [35]).

3.2. X-ray excited luminescence of GAGG:Ce and GAGG:Ce,Mg

The X-ray excited luminescence spectra measured at 9 K with the narrow slits indicate that the Ce^{3+} - related emission band in GAGG:Ce,Mg is slightly shifted to lower energy as compared to GAGG:Ce (Fig. 7a). The same small shift is also observed in the afterglow spectra (Fig. 7b) and in the TSL spectra (Fig. 7c) of these crystals. In principle, this shift could be caused by the presence of Ce^{4+} ions perturbed by Mg^{2+} ions in GAGG:Ce,Mg. However, most probably, the low-energy shift can be explained by smaller Ga content in GAGG:Ce,Mg (x = 2.69) as compared with GAGG:Ce (x = 2.83) (see, e.g., [6,24]).

The intensity of the X-ray excited luminescence in the GAGG:-Ce,Mg crystal is about 1.6 times weaker as compared with the GAGG:Ce crystal.

In the X-ray excited ERL spectrum of GAGG:Ce,Mg, no additional band, which could arise from the recombination of electrons with the Mg^{2+} - stabilized hole O^- centers, was found. Most probably, the electron recombinations with these hole centers are non-radiative.

3.3. Thermally stimulated luminescence of GAGG:Ce and GAGG:Ce,Mg

Unlike the photo- and radioluminescence characteristics, the characteristics of thermally stimulated luminescence of GAGG:Ce and GAGG:Ce,Mg are found to be strongly different (Figs. 8 and 9). The TSL glow curves of the X-ray irradiated at 9 K GAGG:Ce,Mg (solid line) and GAGG:Ce (dashed line) single crystals measured at the same conditions in the 9−300 K temperature range are presented in Fig. 8. For GAGG:Ce, the TSL glow curve is similar to that reported in Refs. [9,10,13]. It is evident that the co-doping of GAGG:Ce with Mg results in the drastic decrease of the TSL intensity, especially in the 140−250 K temperature range. In GAGG:Ce,Mg, the total TSL intensity is by about 1 to 2 orders of magnitude weaker than that in GAGG:Ce. Both in the GAGG:Ce and GAGG:Ce,Mg crystals, the most intense is the broad complex lowest-temperature TSL peak located around 77 K with a shoulder around 175 K. In all the TSL peaks, only the Ce^{3+} - related luminescence is observed (Fig. 7c). No additional emission band, which could arise from the recombination of electrons with the {O^- - Mg^{2+}} - type hole centers, was found in the TSL spectrum of GAGG:Ce,Mg.

Previous studies (see, e.g., [14,23]) have shown that the 5d$_2$ excited level of Ce^{3+} is located inside the conduction band of GAGG. For the 5d$_1$ excited level, different positions with respect to the CB, have been reported depending on the Ga content [5,6,14,23]. Under UV irradiation of the crystals at 90 K in the 4f − 5d$_2$ absorption band of Ce^{3+} ($E_{exc} = 3.6$ eV) the electrons, optically released to the CB, become trapped at different traps. The thermally stimulated release of the trapped electrons results in the appearance of the electron recombination luminescence. The same processes take place under irradiation at 295 K in the 4f - 5d$_1$ absorption band ($E_{exc} = 2.74$ eV).

After UV irradiation of the investigated crystals at 90 K in the 4f − 5d$_2$ absorption band of Ce^{3+}, the afterglow is observed. Its intensity in GAGG:Ce,Mg is about 40 times weaker than that in GAGG:Ce.

The TSL glow curves of the GAGG:Ce,Mg (solid line) and GAGG:Ce (dashed line) single crystals irradiated in the 4f − 5d$_2$

Table 2
TSL characteristics of the GAGG:Ce and GAGG:Ce, Mg single crystals and the GAGG:Ce epitaxial film, see Figs. 9 and 11.

TSL peak, K (T_{irr} = 90 K)	Relative intensity	Trap depth, eV	Frequency factor, s^{-1}
GAGG:Ce crystal			
113	140	0.20 ± 0.01	$\sim 10^7$
150	8	0.40 ± 0.02	$\sim 10^{12}$
200	7	0.50 ± 0.02	$\sim 10^{11}$
260	6	0.62 ± 0.02	$\sim 10^{10}$
325	5	0.72 ± 0.02	$\sim 10^9$
380	13	0.96 ± 0.02	$\sim 10^{11}$
460	1–2	–	
TSL peak, K (T_{irr} = 295 K)			
325	7	0.88 ± 0.04	$\sim 10^{11}$
378	77	0.97 ± 0.02	$\sim 10^{11}$
460	2–3	0.75 ± 0.05	$\sim 10^6$
GAGG:Ce, Mg crystal			
115	135	0.22 ± 0.01	$\sim 10^8$
160	22	0.43 ± 0.02	$\sim 10^{12}$
200	8	–	
285	70	0.65 ± 0.05	$\sim 10^{10}$
325	~ 20	0.84 ± 0.03	$\sim 10^{11}$
440	8	0.95 ± 0.02	$\sim 10^9$
TSL peak, K (T_{irr} = 295 K)			
325	48	0.87 ± 0.03	$\sim 6 \times 10^{11}$
440	31	0.99 ± 0.03	$\sim 3 \times 10^9$
GAGG:Ce film (5LGB5)			
114	141	0.21 ± 0.01	$\sim 10^8$
140	5	0.30 ± 0.02	$\sim 10^9$
155	4	0.42 ± 0.02	$\sim 10^{12}$
200	3.5	–	
260	37	0.60 ± 0.02	$\sim 10^{10}$
312	19	0.66 ± 0.04	$\sim 10^9$
435	2	–	
TSL peak, K (T_{irr} = 295 K)			
327	49	0.68 ± 0.02	5×10^8
435	4	–	
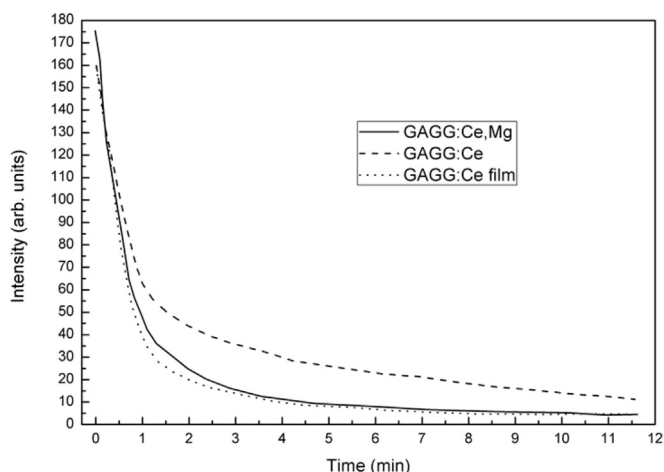
Fig. 10. Dependences of the afterglow intensity on time t measured after the sample irradiation at 90 K with E_{irr} = 3.6 eV (normalized at t = 0.25 min) for the GAGG:Ce,Mg (solid line) and GAGG:Ce (dashed line) single crystals and the GAGG:Ce film (dotted line).

absorption band of Ce^{3+} are compared in Fig. 9. After UV irradiation at 90 K, the most intense complex TSL peak is located around 113–115 K with a weaker shoulder around 150–160 K. In GAGG:Ce,Mg, the intensity of this peak is about 36 times weaker as compared to GAGG:Ce. In GAGG:Ce, much weaker complex TSL peaks are observed around 200 K, 260 K, 325 K, 380 K, and 460 K (see also Table 2). In GAGG:Ce, Mg, the intensity of a new 285 K peak is about two times weaker as compared with the 115 K peak; a new peak is observed also around 440 K. The peak of GAGG:Ce

located around 380 K is completely absent in GAGG:Ce,Mg (see also the inset to Fig. 9).

Thus, unlike GAGG:Ce,Ca, where a new intense peak appears at 390 K with the intensity comparable to that of the main low-temperature TSL peak in GAGG:Ce [5], no such peak is observed in GAGG:Ce,Mg. This indicates much more favourable defect structure in GAGG:Ce,Mg and could be a reason of better scintillation characteristics of GAGG:Ce,Mg as compared with GAGG:-Ce,Ca (see Ref. [15]).

For comparison, the TSL glow curve of the GAGG:Ce epitaxial film of similar composition (5LGB5), measured in Ref. [23] after irradiation of the film in the 4f - $5d_2$ absorption band of Ce^{3+}, is also presented in Fig. 9 (dotted line). It is interesting to note that the absolute values of the afterglow and the TSL intensity in the GAGG:Ce film and the GAGG:Ce,Mg crystal are comparable. The peak at about 380 K is absent also in the GAGG:Ce film. The afterglow decay kinetics are similar as well. Indeed, in both these samples, the afterglow decays much more quickly as compared with the GAGG:Ce single crystal (Fig. 10). These data indicate that not only the decrease of the preparation temperature but also the co-doping with Mg^{2+} can strongly affect the defect structure in GAGG:Ce. Similar conclusion was made in Ref. [29] on the influence of Mg^{2+} on the defect structure in $Lu_3Al_5O_{12}$:Ce.

From the TSL data, the parameters of the traps (trap depths E_t and frequency factors f_0) corresponding to each TSL can be determined. In the 8–125 K temperature range, the E_t values are obtained using fractional glow technique [32], see Fig. 8b. In the 90–500 K temperature range, the E_t values are obtained by the partial cleaning method (for more details, see, e.g. [31], and references therein) from the slope of the $lnI_{TSL}(1/T)$ dependences after heating of the irradiated sample up to the selected temperatures T_{stop}. In Fig. 11, the dependences of the trap depths E_t on the
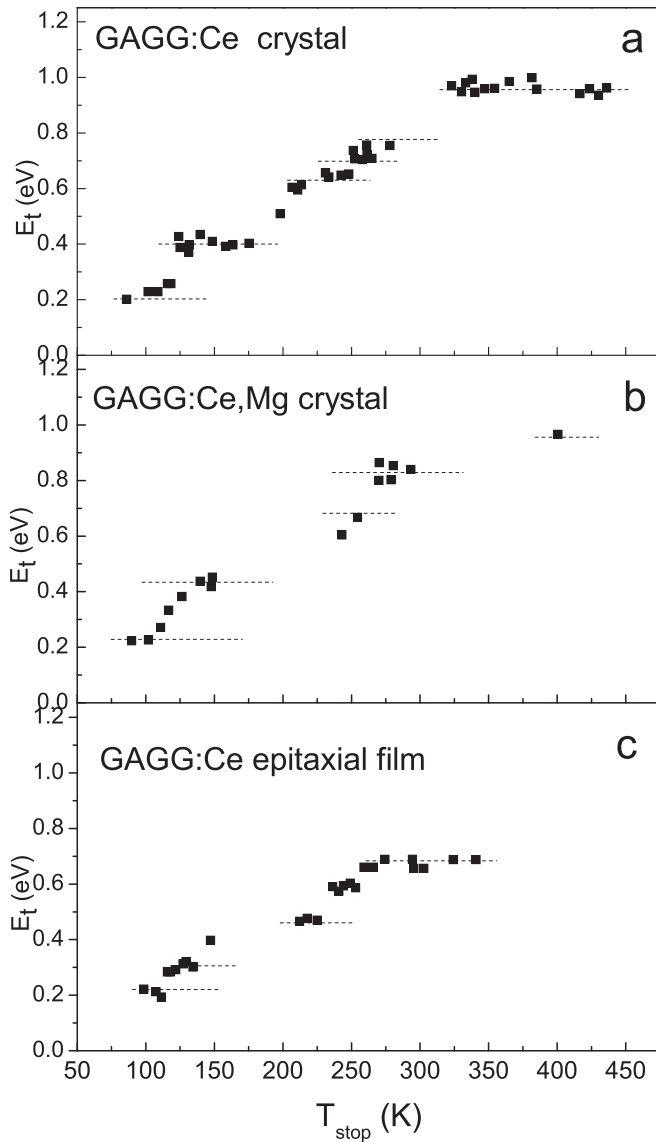
Fig. 11. Dependences of the trap depths E_t, corresponding to different TSL glow curve peaks, on the temperature T_{stop} obtained for the (a) GAGG:Ce and (b) GAGG:Ce,Mg single crystals and (c) the GAGG:Ce epitaxial film irradiated at 90 K in the $4f - 5d_2$ absorption band of Ce^{3+}.

Fig. 12. The ln $I_{TSL} - 1/T_{irr}$ dependences measured for the GAGG:Ce crystal (for the TSL peak at 380 K), the GAGG:Ce,Mg crystal (for the TSL peaks at 285 K and 440 K), and the GAGG:Ce epitaxial film (for the TSL peak at 325 K) irradiated in the Ce^{3+} - related 4f - $5d_1$ absorption band.

temperature T_{stop} are presented for the GAGG:Ce and GAGG:Ce,Mg single crystals and the GAGG:Ce film (see also Table 2). In case of the first-order recombination kinetics characteristic for GAGG:Ce (see, e.g., [9,10,13]), the frequency factors f_0 can be calculated using the expression

$$f_0 = \left(\beta E_t / kT_m^2 \right) \exp(E_t/kT_m), \qquad (2)$$

where β is the crystal heating rate, k is the Boltzmann factor, and T_m is the maximum position of the considered TSL peak. Due to a complex structure of the TSL peaks, only approximate values of the E_t and f_0 parameters could be obtained. The T_m value is taken as the temperature where the peak position becomes independent of T_{stop}. According to our estimations, T_m values for the main TSL peaks can be defined with an accuracy of about 2—5 K. The values of E_t are defined with an accuracy of about 5—10%. For the f_0 values, only an order of magnitude can be roughly estimated (Table 2).
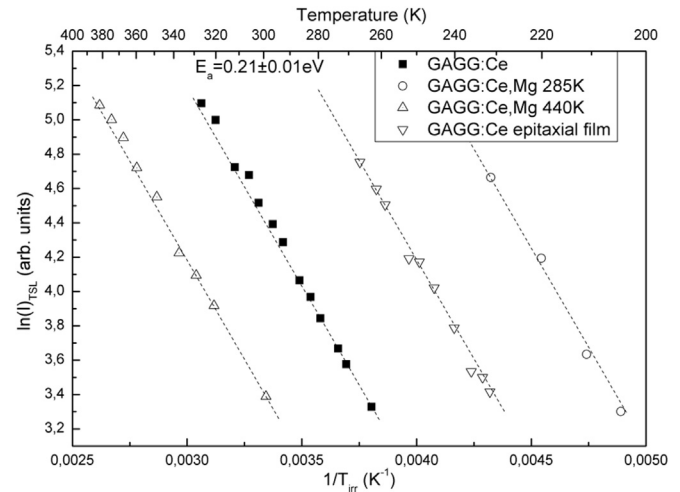
It is evident, that the E_t values for the TSL peaks located in the T < 230 K temperature range are not much influenced by the Mg^{2+} co-doping and the preparation temperature of GAGG:Ce. This indicates the similar origin of the corresponding traps in all the samples studied. Based on presented data we suggest that the electron traps, responsible for the TSL peaks located in the 150—230 K range, can be caused by the antisite defects. The complex TSL peak around 285 K, arising from the traps with $E_t \approx 0.65$ eV, is characteristic for the GAGG:Ce,Mg crystal and, most probably, arises from a Mg^{2+} - containing defect. The lower-temperature part of this peak can arise from a hole trapped at an oxygen ion located close to a Mg^{2+} ion (the {O^- - Mg^{2+}} - type hole centre). As it was mentioned above, these centers are detected only in the Mg^{2+} - containing $Lu_3Al_5O_{12}$:Ce where they are stable up to 280 K [30]. The room temperature afterglow of GAGG:Ce,Mg arises from the recombination of the defects responsible for the ≈ 285 K peak. The peak at 380 K with $E_t \approx 0.96$ eV, characteristic only for the GAGG:Ce single crystal, is most probably connected with a single oxygen vacancy. Relatively small value of the trap depth ($E_t \approx 0.75$ eV) and the corresponding frequency factor ($f_0 \sim 10^6$ s^{-1}) obtained for the TSL peak at 460 K indicate the hole origin of this peak. Indeed, in Ref. [36], the f_0 values for the hole trap related TSL glow curve peaks were found to be by 2—3 orders of magnitude smaller as compared to the close electron trap related TSL peaks. It is not excluded that the peak at about 440 K in GAGG:Ce,Mg is also of a hole origin.

From the dependence of the TSL peak intensity on the irradiation temperature T_{irr} (Fig. 12), the activation energy E_a was determined for the TSL peaks formation. Taking into account the data of [14], we expected to obtain the smaller E_a value for GAGG:Ce,Mg as compared with GAGG:Ce. However, the E_a values, indicating the position of the $5d_1$ excited level of Ce^{3+} with respect to the bottom of the CB, are very close in the GAGG:Ce and GAGG:Ce,Mg crystals ($E_a = 0.21 \pm 0.01$ eV and $E_a = 0.22 \pm 0.01$ eV, respectively). It should also be noted that at the temperature dependence of the $5d_1 - 4f$ luminescence intensity (Fig. 2), the stage with the activation energy $E_q \approx 0.21$—0.22 eV, caused by the thermally stimulated transitions of the electron from the $5d_1$ excited level of Ce^{3+} to the CB, is also observed but only in the small temperature range between 360 K and 400 K.

A small difference in the E_a values observed for the investigated

GAGG:Ce and GAGG:Ce, Mg crystals can be caused by slightly different Ga contents in these two crystals (x = 2.831 and x = 2.694, respectively) (for more details, see Ref. [23]). Therefore, strongly different activation energies of the luminescence thermal quenching reported for GAGG:Ce and GAGG:Ce,Ca in Ref. [14] are most probably caused by different Ga contents in these crystals.

4. Conclusions

Unlike the scintillation characteristics, where the substantial shortening of both the rise time and the decay time has been observed in Ref. [19], no noticeable influence of Mg^{2+} on the photo- and X-ray excited luminescence characteristics of GAGG:Ce single crystals is found in this work. Under photoexcitation in the Ce^{3+} - and Gd^{3+} - related absorption bands, no rise of the photo-luminescence intensity in time with the rise time value above 1 nanosecond is observed neither in GAGG:Ce,Mg nor in GAGG:Ce crystals. The position of the $5d_1$ excited level of Ce^{3+} with respect to the conduction band is not influenced by Mg^{2+} as well. These data allow to conclude that Mg^{2+} ions do not noticeably perturb the energy levels of neither Ce^{3+} nor Ce^{4+} ions.

At the same time, the co-doping with Mg^{2+} results not only in the strong reduction of afterglow but also in a drastic decrease of the thermally stimulated luminescence intensity in the whole investigated temperature range (T < 500 K), which indicates a strong decrease of the concentration of intrinsic crystal lattice defects. A positive influence of Mg^{2+} on the TSL characteristics of GAGG:Ce is mainly caused by the formation of Ce^{4+} ions as effective electron traps which successfully compete with the intrinsic electron traps in the crystal lattice of GAGG [19]. Additionally, the co-doping with Mg^{2+} can result in the suppression of the number of single (noncompensated) cation and oxygen vacancies due to the formation of their associates with Ce^{4+} and Mg^{2+} ions, respectively. Indeed, the compensation of the excess charge of the single vacancies can considerably reduce the efficiency of trapping of charge carriers. The formation of the antisite defects of the type of Gd^{3+}_{Ga} or Gd^{3+}_{Al} needs the presence of volume-compensating vacancies due to a strong difference in ionic radii between the Gd^{3+} ion and the Ga^{3+} or Al^{3+} ions. Therefore, the Mg^{2+} - induced suppression of the number of single vacancies might result in the decreasing concentration of the antisite defects as well.

Besides, the Mg^{2+} - induced changes in the defects structure appear also in much faster decay of the afterglow and in the change of the shape of the TSL glow curve. The decrease of the scintillation light yield in GAGG:Ce,Mg as compared to GAGG:Ce can be due to nonradiative recombination of electrons and holes around the O^- - based complex defects.

Thus, the Mg^{2+} - induced changes in the concentration, origin and structure of the impurity and intrinsic defects in the GAGG:Ce crystal lattice lead to both the considerable improvement of the timing performance of GAGG:Ce (due to the formation of Ce^{4+} centers) and decrease of the scintillation light yield (about 1.3 times) reported in Ref. [19]. However, taking into account an extremely high light yield of 58 000 photon/MeV and the energy resolution of 4.2%@662 keV obtained for GAGG:Ce single crystals in Ref. [11], high density of this material (6.63 g/cm^3), excellent timing characteristics, low afterglow, and very good radiation hardness [19], GAGG:Ce,Mg can be considered as a very promising scintillating material for application in medical imaging and high energy physics detectors.

References

[1] K. Kamada, T. Endo, K. Tsutumi, T. Yanagida, Y. Fujimoto, A. Fukabori, A. Yoshikawa, J. Pejchal, M. Nikl, Cryst. Growth Des. 11 (2011) 4484—4490.
[2] K. Kamada, T. Yanagida, T. Endo, K. Tsutumi, Y. Usuki, M. Nikl, Y. Fujimoto, A. Fukabori, A. Yoshikawa, J. Cryst. Growth 352 (2012) 88—90.
[3] K. Kamada, T. Yanagida, J. Pejchal, M. Nikl, T. Endo, K. Tsutsumi, Y. Fujimoto, A. Fukabori, A. Yoshikawa, IEEE Trans. Nucl. Sci. 59 (2012) 2112—2115.
[4] M. Nikl, A. Yoshikawa, K. Kamada, K. Nejezchleb, C.R. Stanek, J.A. Mares, K. Blazek, Prog. Cryst. Growth Charact. Mater. 59 (2013) 47—72.
[5] M. Tyagi, F. Meng, M. Koschan, S.B. Donnald, H. Rothfuss, C.L. Melcher, J. Phys. D. Appl. Phys. 46 (2013) 475302.
[6] J.M. Ogieglo, A. Katelnikovas, A. Zych, T. Justel, A. Meijerink, C.R. Ronda, J. Phys. Chem. A 117 (2013) 2479—2484.
[7] O. Sakthong, W. Chewpraditkul, Ch. Wanarak, J. Pejchal, K. Kamada, A. Yoshikawa, G.P. Pazzi, M. Nikl, Opt. Mater. 36 (2013) 568—571.
[8] T. Yanagida, K. Kamada, Y. Fujimoto, H. Yagi, T. Yanagitani, Opt. Mater. 35 (2013) 2480—2485.
[9] W. Drozdowski, K. Brylev, M.E. Witkowski, A.J. Wojtowicz, P. Solarz, K. Kamada, A. Yoshikawa, Opt. Mater. 36 (2014) 1665—1669.
[10] K. Brylew, W. Drozdowski, A.J. Wojtowicz, K. Kamada, A. Yoshikawa, J. Lumin. 154 (2014) 452—457.
[11] K. Kamada, S. Kurosawa, P. Prusa, M. Nikl, V.V. Kochurikhin, T. Endo, K. Tsutumi, H. Sato, Y. Yokota, K. Sugiyama, A. Yoshikawa, Opt. Mater. 36 (2014) 1942—1945.
[12] O. Sakthong, W. Chewpraditkul, Ch. Wanarak, K. Kamada, A. Yoshikawa, P. Prusa, M. Nikl, Nucl. Instr. Meth. Phys. Res. A 751 (2014) 1—5.
[13] M. Kitaura, A. Sato, K. Kamada, A. Ohnishi, M. Sasaki, J. Appl. Phys. 115 (2014) 083517.
[14] Y. Wu, F. Meng, Q. Li, M. Koschan, C.L. Melcher, Phys. Rev. Appl. 2 (2014) 044009.
[15] K. Kamada, M. Nikl, S. Kurosawa, A. Beitlerova, A. Nagura, Y. Shoji, J. Pejchal, Y. Ohashi, Y. Yokota, A. Yoshikawa, Opt. Mater. 41 (2015) 63—66.
[16] M. Kitaura, A. Sato, K. Kamada, S. Kurosawa, A. Ohnishi, M. Sasaki, K. Hara, Opt. Mater. 41 (2015) 45—48.
[17] P. Sibczynski, J. Iwanowska-Hanke, M. Moszynski, L. Swiderski, M. Szawlowski, M. Grodzicka, T. Szczesniak, K. Kamada, A. Yoshikawa, Nucl. Instr. Meth. Phys. Res. A 772 (2015) 112—117.
[18] P. Kučera, J.A. Mares, Z. Onderisinova, M. Hanus, V. Babin, A. Beitlerova, M. Nikl, Cryst. Growth Des. 15 (2015) 3715—3723.
[19] M.T. Lucchini, V. Babin, P. Bohacek, S. Gundacker, K. Kamada, M. Nikl, A. Petrosyan, A. Yoshikawa, E. Auffray, Nucl. Instr. Meth. Phys. Res. A 816 (2016) 176—183.
[20] A. Yoshikawa, K. Kamada, S. Kurosawa, Y. Shoji, Y. Yokota, V.I. Chani, J. Lumin. 169 (2016) 387—393.
[21] M. Kitaura, K. Kamada, S. Kurosawa, J. Azuma, A. Ohnishi, A. Yamaji, K. Hara, Appl. Phys. Express 9 (2016) 072602.
[22] K. Kamada, Y. Shoji, V.V. Kochurikhin, A. Nagura, S. Okumura, S. Yamamoto, J.Y. Yeom, S. Kurosawa, J. Pejchal, Y. Yokota, Y. Ohashi, M. Nikl, M. Yoshino, A. Yoshikawa, IEEE Trans. Nucl. Sci. 63 (2016) 443—447.
[23] V. Babin, A. Krasnikov, M. Kučera, M. Nikl, S. Zazubovich, Opt. Mater. 62 (2016) 465—474.
[24] V. Babin, K. Chernenko, M. Kučera, M. Nikl, S. Zazubovich, J. Lumin. 179 (2016) 487—495.
[25] M. Nikl, E. Mihokova, J. Pejchal, A. Vedda, Yu. Zorenko, K. Nejezchleb, Phys. Status Solidi B 242 (2005) R119—R121.
[26] Yu. Zorenko, V. Gorbenko, I. Konstankevych, A. Voloshinovskii, G. Stryganyuk, V. Mikhailin, V. Kolobanov, D. Spassky, J. Lumin. 114 (2005) 85—94.
[27] H. Przybylinska, A. Wittlin, Chong-Geng Ma, M.G. Brik, A. Kaminska, P. Sybilski, Yu. Zorenko, M. Nikl, V. Gorbenko, A. Fedorov, M. Kučera, A. Suchocki, Opt. Mater. 36 (2014) 1515—1519.
[28] T. Kärner, V.V. Laguta, M. Nikl, T. Shalapska, S. Zazubovich, J. Phys. D. Appl. Phys. 47 (2014) 065303.
[29] S. Liu, X. Feng, Z. Zhou, M. Nikl, Y. Shi, Y. Pan, Phys. Status Solidi RRL 8 (2014) 105—109.
[30] C. Hu, S. Liu, M. Fasoli, A. Vedda, M. Nikl, X. Feng, Y. Pan, Phys. Status Solidi RRL 9 (2015) 245—249. Opt. Mater. 45(2015) 252—257.
[31] A. Vedda, M. Nikl, M. Fasoli, E. Mihokova, J. Pechal, M. Dusek, G. Ren, C.R. Stanek, K.J. McClellan, D.D. Byler, Phys. Rev. B 78 (2008) 195123.
[32] R. Chen, S.W.S. McKeever, Theory of Thermoluminescence and Related Phenomena, World Scientific Pub. Co., 1997.
[33] P. Dorenbos, J. Lumin. 134 (2013) 310—318.
[34] V. Babin, M. Nikl, K. Kamada, A. Beitlerova, A. Yoshikawa, J. Phys. D. Appl. Phys. 46 (2013) 365303.
[35] K. Bartosiewicz, V. Babin, K. Kamada, A. Yoshikawa, M. Nikl, J. Lumin. 166 (2015) 117—122.
[36] T. Kärner, V. Laguta, M. Nikl, S. Zazubovich, Phys. Status. Solidi B 251 (2014) 741—747.
[37] V. Jary, A. Krasnikov, M. Nikl, S. Zazubovich, Phys. Status Solidi B 252 (2015), 274—271.